Modeling and Simulation of Cadmium Removal from the Groundwater by Permeable Reactive Barrier Technology

Dr. Ayad Abdulhamza Faisal
Assistant Professor
College of Engineering-University of Baghdad
e-mail: ayadabedalhamzafaisal@yahoo.com

Zaman Ageel Hmood
MSc. student
College of Engineering- University of Baghdad
e-mail: aube_z@yahoo.com

ABSTRACT

The removal of cadmium ions from simulated groundwater by zeolite permeable reactive barrier was investigated. Batch tests have been performed to characterize the equilibrium sorption properties of the zeolite in cadmium-containing aqueous solutions. Many operating parameters such as contact time, initial pH of solution, initial concentration, resin dosage and agitation speed were investigated. The best values of these parameters that will achieved removal efficiency of cadmium (=99.5%) were 60 min, 6.5, 50 mg/L, 0.25 g/100 ml and 270 rpm respectively. A 1D explicit finite difference model has been developed to describe pollutant transport within a groundwater taking the pollutant sorption on the permeable reactive barrier (PRB), which is performed by Langmuir equation, into account. Computer program written in MATLAB R2009b successfully predicted meaningful values for Cd^{+2} concentration profiles. Numerical results show that the PRB starts to saturate after a period of time (~120 h) due to reduce of the retardation factor, indicating a decrease in percentage of zeolite functionality. However, a reasonable agreement between model predictions and experimental results of the total concentration distribution of Cd^{2+} species across the soil bed in the presence of zeolite permeable reactive barrier was recognized.

Keywords: cadmium removal, sorption process, zeolite, permeable barrier, groundwater remediation.

نمذجة ومحاكاة معالجة المياه الجوفيه الملوثه بالكادميوم باستخدام تقنيه الحاجزالتفاعلي النفاذ

د.أياد عبد الحمزه
أستاذ مساعد
كلية الهندسة- جامعة بغداد

زمن عجيل حمود
طالبة ماجستير
كلية الهندسة-جامعة بغداد

الخلاصة

ازالة ايونات الكادميوم من المياه الجوفيه باستخدام حاجز تفاعلي نفاذ من الزيولايت تم النحري عنها بالدراسة الحالية. حيث اجريت العديد من فحوصات الدفعة لتوصيف خواص امتزاز ملوث الكادميوم من المحاليل المائية على مادة الزيولايت. تم دراسة تأثيرالعديد من المتغيرات التشغيليه مثل زمن التماس، الداله الحامضية الابتدائية للمحلول، التركيز الابتدائي للمعدن، كمية الماده المازة وسرعة الاهتزاز. ان افضل قيم لتلك المتغيرات والتي تحقق كفاءة ازالة لملوث الكادميوم تصل الى 99.5% كانت 60 دقيقه، 6.5، 50 ملغم/لتر،0.25 ملغم/100مليلتر و 270 دورة/دقيقه على التوالي.تم اعداد نموذج رياضي احادي البعد باستخدام طريقة الفروق المحددة والذي يأخذ الامتزاز الحاصل في منطقة الحاجز التفاعلي النفاذ بواسطة معادلة لانكمير بنظر الاعتبار. ومن ثم استخدام برنامج الماتلاب والذي استطاع ان يعبر بنجاح عن ذلك النموذج والذي يهدف الى رسم قيم تراكيز الكادميوم زمانيا ومكانيا. أظهرت النتائج العددية بدء عملية تشبع الحاجز الفعال النفاذ بعد فتره زمنية تصل الى (120ساعه) بفعل تناقص معامل الاحتجاز والذي يشير الى تناقص الاداء لذلك الحاجز. على العموم يوجد تطابق بين النتائج النظرية والنتائج المختبرية لتوزيع تراكيز الكادميوم على طول التربه الملوثه بوجود الزيولايت كحاجز تفاعلي نفاذ.

1. INTRODUCTION

The presence of toxic pollutants in groundwater brings about significant changes in the properties of water resources and has to be avoided in order to preserve the environmental quality. Heavy metals are among the most dangerous inorganic water pollutants, they can be related to many anthropogenic sources and their compounds are extremely toxic. Many heavy metals, such as mercury, chromium and cadmium, accumulate in the aquatic food web reaching human beings through the food chain, and causing several pathologies. The presence of heavy metals in groundwater is due to water exchange with contaminated rivers and lakes or to leaching from contaminated soils by rainfall infiltration.

Groundwater remediation techniques such as pump and treat are widely used but have proven that they are difficult, costly and ineffective most of the time in removing enough contamination to restore the groundwater to drinking water standards in acceptable time frames. The primary reason for the failure of pump and treat is the inability to extract contaminants from the subsurface due to hydro-geologic factors and trapped residual contaminant mass. Hence, the removal of these contaminants from groundwater is a major challenge for environmental engineering. One of the most promising technologies is the in-situ treatment of groundwater contaminants by means of permeable reactive or adsorbing barriers (PRBs)**, Di Natale, et al., 2008.**

The main advantage of a reactive barrier is the passive nature of the treatment: the contaminated groundwater moves under natural hydraulic gradient through the permeable reactive zone where the pollutant is degraded or immobilized. The use of reactive materials whose hydraulic conductivity is higher than that of the surrounding soils ensures that groundwater spontaneously flows through the barrier without any external energy input. This method is found to be more cost-effective than pump and treat and has been a demonstrated potential to diminish the spread of contaminants which have proven difficult and expensive to manage with other cleanup methods**, Puls, et al., 1998**.

Accordingly, PRBs are installed in the aquifer across the flow path of a contaminant plume. As the contaminated groundwater moves through these barriers due to the natural gradient, the contaminants are removed by physical, chemical and/or biological processes. Depending on what processes take place, the reactive barrier material can remain permanently in the subsurface, or replaceable units can be provided. As the reactions that occur in such systems are affected by many parameters, successful application of this technology requires a sufficient of contaminants characterization**, Stengele, and Kohler, 2001**.

2. THEORY

A general differential equation, describing the transport of a dissolved constituent, subject to physical and chemical transport processes. The mass conservation equation for control volume shown in **Fig. 1** may be expressed as**:**

(Rate of mass input) - (rate of mass output) ± (rate of mass production or consumption) = rate of mass accumulation (1)

This equation can be written mathematically as:

$$-\left[\frac{\partial J_x}{\partial x}+\frac{\partial J_y}{\partial y}+\frac{\partial J_z}{\partial z}\right]\pm r=\frac{\partial(nc)}{\partial t} \quad (2)$$

where J is the mass flux of solute per unit cross-sectional area transported in the direction indicated by the subscript x, y, or z; r is the rate of mass production/consumption given by the

kinetic model of reaction, *n* is the porosity of the medium, and *c* is the solute concentration expressed as mass of solute per unit volume of solution.

The two mass transport processes of advection and dispersion govern *J* in **Eq. (2).** The transport of dissolved contaminants follows that of water via advection and is therefore related to the velocity of water flow. The direction of hydraulic gradients dictates to a large extent the direction of dissolved contaminant transport. If advection is the only mechanism of transport, the pore velocity (Darcy velocity divided by porosity) is an indicator of the transport of dissolved contaminants. In reality, however, there are other mechanisms incorporating with advection. The saturated soil possesses concentration gradients in addition to hydraulic gradients because of the localized presence of the dissolved chemical. These concentration gradients provide an additional mechanism of transport namely, diffusion. The effect of diffusion is represented by spread out of contaminant in all directions in response to concentration gradients. The relative contributions of advection and diffusion are therefore dependent on the magnitudes of velocity and the concentration gradients. The diffusion of chemicals in soils is typically grouped with another important transport mechanism known as mechanical dispersion. The mechanical dispersion is the effect of advective velocities which, when sufficiently high, cause a mixing of the chemical in the porous medium. Accordingly, the mass flux (*J*) due to advection and dispersion in the *x* direction may be expressed as**, Reddi, and Inyang, 2000**:

$$J_{advection} = V_x nc \quad \& \quad J_{dispersion} = -nD_x \frac{\partial c}{\partial x} \tag{3}$$

where V_x is pore velocity in the *x* direction. The D_x includes the two components of molecular diffusion and mechanical dispersion. Summing up the contributions from advection and dispersion, the mass fluxes are substituted into the **Eq. (2)** and the resultant will be:

$$-\left[\frac{\partial}{\partial x}\left(V_x nc - nD_x \frac{\partial c}{\partial x}\right)\right] - \left[\frac{\partial}{\partial y}\left(V_y nc - nD_y \frac{\partial c}{\partial y}\right)\right] - \left[\frac{\partial}{\partial z}\left(V_z nc - nD_z \frac{\partial c}{\partial z}\right)\right] \pm r = \frac{\partial (nc)}{\partial t} \tag{4}$$

By assuming that the velocities are steady and uniform, the dispersion coefficients do not vary in space, and the porosity of the medium is constant in time and space; one dimensional mass transport of solute in the saturated zone of the soil which well-known advection-dispersion equation (ADE) can be established as follows:

$$D_z \frac{\partial^2 c}{\partial z^2} - V_z \frac{\partial c}{\partial z} \pm \frac{r}{n} = \frac{\partial c}{\partial t} \tag{5}$$

The exact form of the ADE depends on the mass transfer processes accounted for in the term *r*. One of the dominant mass transfer mechanisms occurring during mass transport is sorption which represents the fundamental mechanism for the operation of the reactive permeable barriers. Incorporating sorption can be achieved by using Linear, Langmuir, or Freundlich isotherm. However, the simplest way for incorporation is the linear sorption isotherm as below:

$$S = K_d c \tag{6}$$

where *S* is the quantity of mass sorbed on the surface of solids and K_d is the distribution coefficient. The rate expression *r* is equal to the product of time derivative of *S* and dry mass density, ρ_b. Thus,

$$r = \rho_b \frac{\partial S}{\partial t} = K_d \rho_b \frac{\partial c}{\partial t} \quad (7)$$

Substituting **Eq. (7)** in the **Eq. (5)** and rearrangement of terms yields:

$$D_z \frac{\partial^2 c}{\partial z^2} - V_z \frac{\partial c}{\partial z} = R \frac{\partial c}{\partial t} \quad (8)$$

where R ($=1+\rho_b K_d / n$) is known as the retardation factor since it has the effect of retarding the transport of adsorbed species relative to the advection front.

3. BOUNDARY VALUE PROBLEM

3.1 Governing Equations

The 1D model consists of the source area (where the aqueous-phase source is assumed to be perfectly mixed and the concentration, c_s, is assumed to be uniform) and two homogenous porous transport domains; the receiving aquifer and the permeable reactive barrier as shown in **Fig. 2.** Because the reactive barrier is permeable, flow velocity (V_B) in the barrier is evaluated as follows:

$$V_A n_A = V_B n_B \quad (9)$$

where n_A is the porosity of the aquifer; n_B is the porosity of the barrier; and V_A is the flow velocity in the aquifer. **Eq. (8)** can be re-written to describe the contaminant, i.e. Cd^{2+}, transport inside the barrier as follows:

$$D_{Bz} \frac{\partial^2 c_{CdB}}{\partial z^2} - V_{Bz} \frac{\partial c_{CdB}}{\partial z} = R_B \frac{\partial c_{CdB}}{\partial t} \quad (10)$$

where c_{CdB} is the cadmium concentration in the permeable reactive barrier for $L_A \le z \le L_A+L_B$; D_{Bz} is the reactive barrier molecular dispersion coefficient in the direction of flow and R_B is the retardation factor in the barrier. In the same manner, solute transport in the aquifer can be written as:

$$D_{Az} \frac{\partial^2 c_{CdA}}{\partial z^2} - V_{Az} \frac{\partial c_{CdA}}{\partial z} = R_A \frac{\partial c_{CdA}}{\partial t} \quad (11)$$

where c_{CdA} is the cadmium concentration in the aquifer for $0 \le z \le L_A$ and $L_A+L_B \le z \le L$; D_{Az} is the hydrodynamic dispersion coefficient and R_A is the retardation factor in the aquifer. However, the value of R_A is assumed equal to 1 in the present study. Also, continuity is assumed at the reactive barrier- aquifer interface.

3.2 Initial and Boundary Conditions

The mathematical model consists of the three governing differential equations describing cadmium transport in the aquifer upstream of the barrier, in the barrier, and in the aquifer downstream of the barrier **Eqs. (10)** and **(11**). Each equation in each domain must have one initial and two boundary conditions to generate the required solution describing the contaminant distribution as function of distance and time. The initial conditions:

$c_{CdA}(z,0) = 0$ for $0 \le z \le L_A$ and $L_A+L_B \le z \le L$ (12a)

$c_{CdB}(z,0) = 0$ $L_A \le z \le L_A+L_B$ (12b)

Also, two boundary conditions and four intermediate conditions at the interface between the barrier and the aquifer are selected to complete the solution process as follows:

$c_{CdA}(0,t)=c_s$ (13a)

$$\frac{\partial c_{cdA}}{\partial z} = 0 \qquad @\ (L,t) \tag{13b}$$

$c_{CdA}(L_A,t)=c_{CdB}(L_A,t)$ (13c)

$c_{CdA}(L_A+L_B,t)=c_{CdB}(L_A+L_B,t)$ (13d)

$$-D_{Bz}n_B\frac{\partial c_{CdB}}{\partial z} + V_{Bz}n_B c_{CdB} = -D_{Az}n_A\frac{\partial c_{CdA}}{\partial z} + V_{Az}n_A c_{CdA} \qquad @\ (L_A\ ,\ t) \tag{13e}$$

$$-D_B n_B\frac{\partial c_B}{\partial x} + V_B n_B C_B = -D_A n_A\frac{\partial c_A}{\partial x} + V_A n_A C_A \qquad @\ (L_A+L_B,\ t) \tag{13f}$$

where L_A is the distance from source of contaminant to the reactive barrier and L_B is the thickness of the reactive barrier.

An explicit method among finite difference methods was applied to the PDE describing the transport of contaminant through saturated zone of the soil. **Eq. (10)** was formulated with the following producer: for time, forward difference was used; for space, backward difference was used for simple partial difference; and center difference was used for quadratic partial difference:

$$c_{CdB_i}^{n+1} = c_{CdB_i}^{n} + \left(\frac{\Delta t}{R_B}\right)(D_{Bz})\left(\frac{c_{CdB_{i-1}}^{n} - 2c_{CdB_i}^{n} + c_{CdB_{i+1}}^{n}}{(\Delta z)^2}\right) - \left(\frac{\Delta t}{R_B}\right)(V_{Bz})\left(\frac{c_{CdB_i}^{n} - c_{CdB_{i-1}}^{n}}{\Delta z}\right) \tag{14}$$

This equation can be re-written as a following simple form:

$$c_{CdB_i}^{n+1} = e_i c_{CdB_{i-1}}^{n} + a_i c_{HCdB_i}^{n} + b_i c_{CdB_{i+1}}^{n} \tag{15}$$

$$e_i = \left[\frac{D_{Bz}(\Delta t)}{R_B(\Delta z)^2} + \frac{V_{Bz}(\Delta t)}{R_B(\Delta z)}\right]$$

$$a_i = \left[1 - 2\frac{D_{Bz}(\Delta t)}{R_B(\Delta z)^2} - \frac{V_{Bz}(\Delta t)}{R_B(\Delta z)}\right]$$

$$b_i = \left[\frac{D_{Bz}(\Delta t)}{R_B(\Delta z)^2}\right]$$

where e_i a_i, and b_i are the coefficients associated with $c_{Cd_{i-1}}^{n}$,$c_{Cd_i}^{n}$ &$c_{Cd_{i+1}}^{n}$, respectively. The superscript n+1 and n are the next and present time step, respectively; $\Delta t=^{n+1}$-t^n is the time step size, and *i*, *i*+1, *i*-1 are the grid identification **Fig. 3.**

Similar to **Eq. (10),** the migration of Cd^{2+} through the aquifer domain described by **Eq. (11)** can be formulated in the same procedure. The formulation of discretized algebraic equations was

followed by development of computer program for its implementation. This program was written in MATLAB R2009b.

4. EXPERIMENTAL METHODOLOGY

4.1 Materials

Naturally Iraqi soil was used as porous medium in the experiments conducted in the present study. **Table 1** summaries the composition and properties of this soil. It was cleaning and well-sorted which needed to an additional sieving to achieve satisfactory uniformity. The proper characterization and preparation of the soil was important in order to ensure high accuracy in the experimental procedure.

A commercially zeolite pellets with diameter (35.96 mm) manufactured by (Dwax company for synthetic zeolite) were used as reactive materials. The resins were washed with 1M of NaOH and 1M of HCl in order to remove possible organic impurities, and then they washed with distilled water to remove all excess and basic. Finally the resins were dried for 24 hours. **Table 2** shows the composition and reported physico-chemical properties of the zeolite used in the present study.

Cadmium was selected as a representative of heavy metal contaminants. To simulate the water's cadmium contamination, a solution of $Cd(NO_3)_2.2H_2O$ (manufactured by E. MERCK, Denmark) was prepared and added to the specimen to obtain representative concentration.

4.2 Batch Experiments

Batch equilibrium tests are carried out to specify the best conditions of contact time, pH, initial concentration, resin dosage and agitation speed. This means that these tests are suited to identify the activity of the reactive material and the sorption isotherm. Series of 250 ml flasks are employed. Each flask is filled with 100 ml of cadmium solution which has initial concentration of 50 mg/l. About 0.25 g of adsorbent was added into different flasks. The solution in the each flask was kept stirred in the high-speed orbital shaker at 270 rpm for 3 hours. A fixed volume (20ml) of the solution was withdrawn from each flask. This withdrawn solution was filtered to separate the adsorbent and a fixed volume (10 ml) of the clear solution was pipetted out for the determination of the amount of unsorbed metal ion still present in solution. The measurements were carried out using atomic absorption spectrophotometer (AAS). These measurements were repeated for two times and average value has been taken. However, the adsorbed concentration of metal ion on the resin was obtained by a mass balance.

Kinetic studies were investigated with different values of pH (2, 4, 6.5, and 8), different values of initial concentration of Cd^{2+} (50, 100, 150, 200 and 250 mg/l), five amounts of adsorbent dosage (0.15, 0.25, 0.5, 1 and 2 g) and finally two values of shaking speed (200 and 270 rpm).

4.3 Column Test Setup

Fig. 4 shows the schematic diagram of the reactor setup used in the present study. This setup is constructed of Perspex cylinder having height and diameter equal to 70 and 5 cm, respectively; the column is equipped with seven sampling ports at the distance of 10 (port 1), 20 (port 2), 30 (port 3), 40 (port 4), 50 (port 5), 60 (port 6), 65 cm (port 7) from the bottom. These ports along the length of the column should be constructed of stainless steel fittings which blocked with Viton stoppers. Sampling was carried out at specified periods from sampling ports using needle to be inserted into the center axis of the column.

At the beginning of each test, the column was packed with 45 cm depth of soil specimen measured from the bottom of this column. Then, zeolite with depth of 5 cm was placed at the top

surface of the packed soil. Again, 15 cm of the soil was added above the layer of the zeolite. The column was then filled with distilled water that was fed slowly into the bottom of the column and forced upward through the medium. The up flow column test was performed at constant temperature, 25±1 ºC.

The contaminated solution with Cd^{2+}, which simulated the contaminated groundwater, was introduced into the column from certain reservoir. The flow from this reservoir, which is placed at the elevation higher than the level of column outlet, was controlled by valve 1, flow meter and valve 2. The elevation of water in the reservoir was changed to form the required hydraulic gradient across the specimen and, consequently, this was determining a flow rate within the column. However, three values of flow rate (5, 10, and 15 ml/min) are selected here with corresponding velocities equal to (3.978, 7.958, and 11.937 m/day) respectively. About 11–15 l of artificial contaminated water was flushed the column for each experiment.

Monitoring of Cd^{2+} concentration along the length of the column in the effluent from sampling ports was conducted for a period of 15 hrs. Water samples were taken regularly (after 5, 10, and 15 hours) from these ports. For sampling the ports, three needles were connected to the three ends of Viton stoppers covered port 2, port 4, and port 6 in each test. However, these selected sampling locations may be changed periodically to comprise the ports (1, 3, and 5) during the same test. In addition to specify three locations only for sampling, the column effluent line was closed and a small amount of water (1-1.5 ml) was withdrawn from these ports. In this way, the samples were taken at the flow rate of the column and this minimized disruption of flow within the column. The samples were immediately introduced in poly-ethylene vials and analyzed by AAS.

The filling material in the column was assumed to be homogeneous and incompressible, and constant over time for water-filled porosity. The volumetric water discharge through the column cross section was constant over time and set as the experimental values. The pollutant inlet concentration was set constant. All tubing and fitting for the influent and effluent lines should be composed of an inert material. Information from the column study can be used along with the site characterization and modeling to help in designs the field-scale PRB.

4.4 Hydraulic Parameters Determination

The porosity, *n*, of column was estimated from the weight of the sand soil, M, and the volume of the column, V, according to the following formula:

$$n = 1 - \frac{\rho_b}{\rho_s} \qquad \& \qquad \rho_b = \frac{M}{V} \tag{16}$$

where ρ_b is the bulk density of the soil column and ρ_s is its mass density.

A tracer experiment was performed to determine the effective dispersion coefficient for the system. A sand soil was packed into the column in a dry condition for a depth of 45 cm. The column was then filled with distilled water that was fed slowly into the bottom of the column and forced upward through the medium, pushing the air in front of it. As a result of this procedure, no difficulties with entrapped air were encountered. A solution of 1 g/l NaCl in distilled water as a tracer was continuously fed into the column, at a rate of 0.3 l/hr. Electrical conductivity was measured with time, as a representative of concentration, by using conductivity meter at port 7 (z_o=65 cm). In this case, the value of D_L is given by the following formula**, Ujfaludi, 1986**.

$$D_L = \frac{1}{8}\left[\frac{(z_o - V t_{0.16})}{(t_{0.16})^{0.5}} - \frac{(z_o - V t_{0.84})}{(t_{0.84})^{0.5}}\right]^2 \tag{17}$$

where D_L is the longitudinal dispersion coefficient, V is the mean pore velocity of seepage (volume rate of flow per unit cross sectional area of voids), $t_{0.16}$ and $t_{0.84}$ are the arrival times of $c/c_o = 0.16$ and 0.84 relative concentration values, respectively.

In order to establish the relationship between the D_L and V, the experiment described above was repeated with another two values of flow rate. These values were 0.6 and 0.9 l/hr. However, the same procedure can be adopted to develop the same relationship between the D_L and V when the porous medium will be a zeolite.

.

5. RESULTS AND DISCUSSION

5.1 Batch Experiments

5.1.1 Equilibrium time

Fig. 5 shows the effect of contact time on cadmium exchange using 0.25 g of zeolite added to 100 ml of metal solution for batch tests at 25±1ºC. Equilibrium for the purposes of this study was taken as having been reached when the cadmium removal efficiency values plateau. This occurred at a reaction time of approximately 1 h. This value can be subsequently used for all batch tests.

It is clear from figure mentioned above that the percentage of metal ion sorbed (i.e., adsorption rate) was very fast initially and it's increased with increasing of contact time until reached the equilibrium time. This may be a result to decrease mass transfer coefficient of the diffusion controlled reaction between resins and metal ions**, Zaiter, 2006**. Also this may be due to the presence of large number of resin sites available for the adsorption of metal ions. As the remaining vacant surfaces decreasing, the adsorption rate slowed down due to formation of replusive forces between the metals on the solid surfaces and in the liquid phase**, El-Sayed, et al., 2010.** However, further increase in contact time had no significant effect on cadmium removal. The maximum removal efficiency of cadmium using zeolite achieved in the present study was 99.8%.

5.1.2 Initial pH of the solution

Fig. 6 shows that the sorption behavior of metal ions is more sensitive to pH changes. A general increase in cadmium sorption with increasing pH of the solution has been observed up to pH equal to 6.5. There are no hydroxo complexes in the solution at pH less than 6.5; only dissociated aqua-ion-forming Cd(II) ions are present. Accordingly, the increase in the metal removal as the pH increases (i.e., as the solution becomes more basic) can be explained on the basis of a decrease in competition between proton and metal species for the surface sites, and by the decrease in positive surface charge, which results in a lower columbic repulsion of the sorbing metal. However, further increase in pH values would cause a decreasing in removal efficiency. This may be attributed to the formation of negative cadmium hydroxides $Cd(OH)_2^-$ which are precipitated from the solution making true sorption studies impossible. In addition, at low pH values an excess of protons can compete effectively with the Cd(II) ions for binding sites on zeolite surface.

5.1.3 Initial cadmium concentration

To study the effect of initial concentration of cadmium on the removal efficiency, the operating conditions were set as follows: volumes of solutions used were 100 ml, concentration of cadmium ranging between 50 and 250 mg/l, were shaken with 0.25 g/100 ml of zeolite for 1 h with initial pH of the solution is 6.5.

Fig.7 illustrates the removal of Cd^{2+} ions by zeolite as a function of initial metal ion concentration. The results show that there was a higher removal of the metal in the first values of

initial concentration. This removal was decrease with increasing of initial concentration up to 200 mg/l and beyond this value, there is not a significant change at the amount of adsorbed metal ions. This plateau represents saturation of the active sites available on the zeolite samples for interaction with metal ions. It can be concluded that the amount of metal ions adsorbed into unit mass of the zeolite at equilibrium (the adsorption capacity) rapidly decreases at the low initial metal ions concentration and then it begins to a slight decrease with increasing metal concentration in aqueous solutions in the length between 200 and 250 mg/l. These results indicate that energetically less favorable sites become involved with increasing metal concentrations in the aqueous solution**, Buasri, et al., 2008.**

5.1.4 Resin dose

The dependence of Cd(II) sorption on adsorbent dosage was studied by varying the amount of zeolite from 0.15 to 2 g added to 100 ml of metal solution for batch tests at 25±1ºC, while keeping other parameters as follows; c_o=50 mg/l, pH=6.5, shaking speed=270 rpm and contact time=1 hour. **Fig. 8** presents the Cd(II) removal efficiency as a function of different amounts of zeolite. It can be observed that removal efficiency of the zeolite improved with increasing adsorbent dosage from 0.15 g to 0.25 g for a fixed initial metal concentration. This was expected due to the fact that the higher dose of adsorbents in the solution, the greater availability of exchangeable sites. This also suggests that after a certain dose of adsorbent (0.25 g), the maximum adsorption sets in and hence the amount of Cd(II) bound to the adsorbent and the amount of Cd(II) in solution remains constant even with further addition of the dose of adsorbent.

5.1.5 Agitation speed

Fig. 9 shows that about 77% of the cadmium ions were removed at shaking speed equal to 200 rpm when the contact time at equilibrium and that Cd removal increases with the increase in shaking speed. There was gradual increase in metal ions removal when agitation speed was increased from 200 to 270 rpm at which about 99.5% of Cd ions have been removed at equilibrium time. These results can be associated to the fact that the increase in the agitation speed improves the diffusion of metal ions towards the surface of the adsorbent. Thus, proper contact is developed between metal ions in solution and the binding sites, which promotes effective transfer of sorbate ions to the sorbent sites. **Fig. 9** also shows that optimum equilibrium was reached at the agitation speed of 270 rpm. Therefore, higher uptake of metal ions could be possible at this speed of agitation as it will assure that all the sites are made readily available for metal ions uptake. However, greater availability of functional groups on the surface of adsorbent, which is required for interaction adsorbent and Cd(II), significantly improved the binding capacity and the process proceeded rapidly. This result is important, as the agitation speed and, consequently, the equilibrium time is one of the important parameters for an economical contaminated water treatment system.

5.2 Sorption Isotherms

The Batch Equilibrium Technique (BET) is often used to determine the adsorption characteristics of various materials such as zeolite by plotting their adsorption isotherms. From the experimental results in **Table 3**, the amount of cadmium removed from the solution per gram of zeolite sample (mg/g) can be calculated as follows:

$$q_e = (c_o - c_e)\frac{V}{m} \quad (18)$$

The adsorption isotherms were produced by plotting the amount of heavy metal removed (adsorbed) from the heavy metal solution (q_e in mg/g) against the equilibrium concentration of heavy metal in the solution (c_e in mg/l) at constant temperature. The present data in Table 4 are fitted with linearized form of Langmuir model and the empirical coefficients *a* and *b* may be obtained by plotting c_e/q_e as a function of c_e **Fig. 10**. Also the same data are fitted with linearized form of Freundlich model and the values of K_F and *n* were determined from the slope and intercept of the linear plot of ln q_e versus ln c_e **Fig. 11**.

This means that the values of empirical constant (*a*) and the saturation coefficient (*b*) are 49.5mg/g and 0.29 l/mg respectively. The value of (*a*) is represented the amount of adsorbate adsorbed to form a monolayer coverage on the solid particles which related to the retention capacity of the adsorbent. On the other hand, the value of (*b*) is represented the Langmuir adsorption equilibrium constant. It is related to the binding energy between the adsorbent and the adsorbate. Hence, The Langmuir isotherm equation will be;

$$q_e = \frac{14.355 C_e}{1+0.29 C_e} \quad (19)$$

Also, the values of Freundlich sorption coefficient (K_F) and an empirical constant (1/n) are 26.168 mg/g and 0.13349 respectively. Hence, the Freundlich isotherm equation will be;

$$q_e = 26.168 c_e^{0.13349} \quad (20)$$

The relationship between the adsorbed and the aqueous concentrations at equilibrium has been described by Langmuir and Freundlich isotherms models **Eqs. (19)** and **(20).** The comparison of the experimental values with the values of q_e obtained by these models is shown in **Fig. 12**. As seen from this figure, the fitness between the experimental values and the predicted values using these models were generally very good for all two parameter isotherm models. However, it is clear that the Langmuir isotherm model provided the best correlation (coefficient of determination (R^2) = 0.9887) in compared with Freundlich isotherm model (R^2 = 0.9033) for cadmium adsorption on the zeolite. Accordingly, the Langmuir isotherm model was used to describe the sorption of solute on solid in the partial differential equation governed the transport of a solute undergoing equilibrium sorption through permeable reactive barrier in the continuous mode.

The essential feature of the equation can be expressed in terms of dimensionless separation factor, S_f, defined as:

$$S_f = \frac{1}{1+bC_o} \quad (21)$$

The value of S_f indicates the shape of the isotherm to be unfavorable for S_f >1, linear for S_f =1, favorable for 0< S_f <1, or irreversible for S_f =0**, Bulut, et al., 2008; Hadjmohammadi, et al., 2011**and **Plamondon, et al., 2011.** The variation of S_f with the initial cadmium concentration of the solution is shown in **Fig. 13**.

5.3 Longitudinal Dispersion Coefficient

Results of the experimental runs concerned the measurement of longitudinal dispersion coefficient (D_L) of soil and zeolite are summarized in **Table 4**. Measured values of D_L versus

mean pore velocity (V) obtained with soil particles are shown in **Fig. 14**. While **Fig. 15** shows the relationship between D_L and V for zeolite particles. It is clear that the curves inclined with the horizontal axis. This suggests a linear relationship between the values of D_L and V for sand soil and zeolite as follows:

For soil, $D_L = 9.96678\,V + 0.395667$ R^2=0.993 (22)

For zeolite, $D_L = 17.0019\,V + 0.0033$ R^2=0.9393 (23)

Eqs. (21) and **(22)** are taken the general form of longitudinal hydrodynamic dispersion coefficient as follows:

$$D_L = \alpha_L V + \tau D_o \tag{24}$$

where α_L is the longitudinal dispersivity (cm), τ is the tortuosity and D_o is the molecular diffusion coefficient (cm^2/s). For high velocities the first part dominates, which is the common situation in groundwater, although flow in aquifers is still rather slow compared to fluxes in other hydrological compartments. The proportionality factor between dispersion and velocity along a flow path line is given by the parameter α_L, which has the physical dimension of [length]. One may also use the term dispersion length or longitudinal dispersivity. The subscript 'L' refers to longitudinal, as it is valid only in the direction of the flow. Tortuosity is a measure of the effect of the shape of the flow path followed by water molecules in a porous medium. It is calculated depended on the porosity of the medium (n) as follows:

$$\tau = n^{m-1} \tag{25}$$

Archie (1942) reports values of m; 1.8–2 for consolidated sandstones, 1.3 for unconsolidated sand in a laboratory experiment, and 1.3–2 for partly consolidated sand. For theoretical or conceptual work the value m = 2 is considered, which may be justified if there is no further information as cited by**, Holzbecher, 2007**. The longitudinal dispersivity and the molecular diffusion coefficient can be calculated for sand soil and zeolite ,**Table 5**.

5.4 Cadmium Transport and Adsorption Equations

The equation describes the transport of cadmium through reactive permeable barrier undergoing equilibrium sorption **Eq. (10)** can be re-written as:

$$D_{Bz}\frac{\partial^2 C_{CdB}}{\partial z^2} - V_{Bz}\frac{\partial C_{CdB}}{\partial z} = \frac{\partial C_{cdB}}{\partial t} + \frac{\rho_b}{n_B}\frac{\partial q_e}{\partial t} \tag{26}$$

where c and q_e are the solute concentrations in aqueous and on solid phases, t is the travel time, D is the hydrodynamic dispersion coefficient, V is the mean pore velocity, and z is the travel distance. The sorption of solute on solid is governed by Langmuir sorption isotherm. Combination of these two equations can be explained as:

$$D_{Bz}\frac{\partial^2 C_{CdB}}{\partial z^2} - V_{Bz}\frac{\partial C_{CdB}}{\partial z} = \frac{\partial C_{cdB}}{\partial t} + \frac{\rho_b}{n_B}\frac{\partial\left(\frac{ab\,C_{cdB}}{1+bC_{cdB}}\right)}{\partial t} \tag{27}$$

This equation can be simplified as:

$$D_{Bz}\frac{\partial^2 C_{CdB}}{\partial z^2} - V_{Bz}\frac{\partial C_{CdB}}{\partial z} = \left(1 + \frac{\rho_b}{n_B}\left(\frac{ab}{(1+bC_{cdB})^2}\right)\right)\frac{\partial C_{cdB}}{\partial t} \quad (28)$$

The effect of sorption is to retard the flow of this contaminant. The retardation factor for the Langmuir sorption isotherm, R_L, is expressed in **Eq.(29),** where ρ_b is the bulk density of the adsorbent (g/cm^3), n_B is the porosity of the barrier (=0.34), b (=K_L=0.29) the Langmuir adsorption constant related to the binding energy (l/mg) and a (=q_{max}=49.5) is the maximum amount of solute absorbed by the solid during the batch test (mg/g). Retardation is linked to the adsorption constant; a high value of R_L will give a long retardation and an efficient barrier design. The retardation factor is often calculated to compare the relative migration in contaminant transport and PRB design:

$$R_L = 1 + \frac{\rho_b}{n_B}\left(\frac{ba}{(1+bC_{cdB})^2}\right) \quad (29)$$

The results in **Table 6** showed that retardation reduced with the increase in initial metal concentration, which is often found for other pollutants and adsorbents. A similar trend was found in field tests when studying lithium in a heterogeneous aquifer**, Plamondon, et al., 2011.**

5.5 Model Verification

Parameters and constants related to the sand soil and zeolite adopted for verification of model were evaluated, either through laboratory tests or through approximation using literature data **Table 7**. Porosity and bulk density were experimentally determined. The tortuosity factor (τ) for sand soil modeled was not determined experimentally, but a value of 0.51 for soil and 0.34 for zeolite were used in this study.

Fig. 16 reports the concentration lines of cadmium in the aquifer at different values of contaminated groundwater flow rate after the time interval equal to 0.5 hr. without using PRB. It is clear from this figure that the propagation of contaminated plume is very fast and the time required for reaching the concentration of cadmium in the outlet of column to the constant concentration applied to the lower boundary (i.e., 50 mg/l) is not exceeded 1 h. Also, it seems that the increased value of flow rate will increase the velocity of flow for same cross sectional area of soil specimen and, consequently, this will increase the velocity of cadmium plume propagation. The concentration of the contaminated plume reaching the outlet may attain concentration levels higher than 20 mg/l and largely above the 0.005 mg/l quality limit prescribed for surface waters or drinking water**, Di Natale, et al., 2008.**

After the introduction of the PAB **Fig. 17**, the contaminant plume is hindered by the zeolite and the cadmium concentration level reaching the outlet is around zero after 24 hour for different values of contaminated groundwater flow rate (i.e., 5, 10 and 15 cm^3/min). It is clear from this figure in comparison with **Fig. 16** the important role of zeolite barrier in restriction the propagation of contaminant plume. However, the barrier starts to saturate with increasing the travel time as shown in the **Fig. 18**. This means that the cadmium retardation factor was reduced, indicating a decrease in percentage of zeolite functionality for cadmium retardation. This explains the increase of effluent concentration of cadmium from RPB with increased the travel time.

Many values of zeolite depths such as 10 and 15 cm are applied using numerical model developed here. For column configuration adopted in the present study, the results proved that the depth of zeolite not have any significant effect on distribution of contaminant concentration through the barrier for a given value of flow rate. This means that the equilibrium state was achieved during short period in spite of the optimum contact time calculated from batch tests was 60 min. Accordingly, the zeolite depth applied in the continuous tests was 5 cm.

Comparisons between the predicted and experimental results for cadmium concentration during the migration of the contaminant plume for simulated problem adopted here at different time intervals for specified flow rate are depicted in **Fig. 19**. A reasonable agreement between these results can be observed. These concentrations seem to be almost identical however they are slightly different. The highest percentage of difference encountered between the predicted and experimental concentrations was not exceeded ±20%. However, any variation between the model predictions and experimental results could be attributed to the many causes such as neglecting the salts (such as calcite or carbonate…etc.) adsorption and their adsorption competition with the cadmium over the solid surface (soil and zeolite). The retardation factor of the contaminant on the soil particles assumed equal to 1, i.e. there is no adsorption, in the present study. Also, the competition between the dissolved salts in the groundwater from soil and cadmium are not considered in the present mathematical modeling.

6. CONCLUSIONS

1) The interactions between cadmium ions and zeolite have been investigated. The batch results indicated that several factors such as adsorption or equilibrium time, initial pH of the solution, initial metal ion concentration, resin dose and agitation speed affect the adsorption process. However, the optimum values of these factors will achieve the maximum removal efficiency of Cd^{+2} were 1 hr., 6.5, 50 mg/l, 0.25 g/100 ml, and 270 rpm respectively.

2) The adsorbed amount of cadmium ions can be:

- Increased with increasing pH of the solution up to pH equal to 6.5. However, further increase in pH values would cause a decreasing in removal efficiency. This may be attributed to the formation of negative cadmium hydroxides $Cd(OH)_2^-$ which are precipitated from the solution making true sorption studies impossible.
- Decreased with increasing of initial concentration up to 200 mg/l and beyond this value, there is not a significant change at the amount of adsorbed metal ions. This plateau represents saturation of the active sites available on the zeolite samples for interaction with metal ions.
- Increased with increasing adsorbent dosage from 0.15 g to 0.25 g for a fixed initial metal concentration. This was expected due to the fact that the higher dose of adsorbents in the solution, the greater availability of exchangeable sites.
- Increased with increasing agitation speed from 200 to 270 rpm at which about 99.5% of Cd ions have been removed at equilibrium time. These results can be associated to the fact that the increase in the agitation speed improves the diffusion of metal ions towards the surface of the adsorbent. Thus, proper contact is developed between metal ions in solution and the binding sites, which promotes effective transfer of sorbate ions to the sorbent sites.

3) The experimental equilibrium data obtained were applied to the Langmuir and Freundlich isotherm equations to test the fitness of these equations. The experimental data for cadmium sorption on the zeolite were correlated reasonably well by the Langmuir adsorption isotherm with coefficient of determination (R^2) equal to 0.9887 in compared with Freundlich isotherm model (R^2 = 0.9033). Consequently, the isotherm parameters (q_{max} and K_L) have been calculated and they are equal to 49.5 mg/g and 0.29 l/mg respectively.

4) The dimensionless separation factor (S_f) showed that ion exchange of cadmium ions on zeolite is favorable. The values of S_f are decreased with increasing of initial cadmium concentration. This indicates that ion exchange is more favorable for the higher initial concentration in compared with lower concentration.

5) A 1D numerical model is used to describe pollutant transport within groundwater and the pollutant adsorption on the PRB. The model is applied to a given problem where a PRB is used to restrict the migration of pollutant dissolved in an inflowing groundwater contaminated by the mobilization of Cd(II). Numerical results showed that the PRB starts to saturate after a period of time (~120 hr) due to reduce of the retardation factor, indicating a decrease in percentage of zeolite functionality. However, a reasonable agreement between model predictions and experimental results of the total concentration distribution of Cd^{2+} species across the soil bed was recognized.

REFERENCES

Buasri, A., Yongbut, P., Chaiyut, N., and Phattarasirichot, K., 2008, *Adsorption Equilibrium of Zinc Ions from Aqueous Solution by Using Modified Clinoptilolite*, Chiang Mai J. Sci., Vol. 35, No. 1, PP. 56-62.

Bulut, E., Ozacar, M., and Sengil, I. A., 2008, *Equilibrium and Kinetic Data and Process Design for Adsorption of Congo Red on to Bentonite*, Journal of Hazardous Materials, Vol. 154, PP. 613-622.

Di Natale, F., Di Natale, M., Greco, R., Lancia, A., Laudante, C., and Musmarra, D., 2008, *Groundwater Protection from Cadmium Contamination by Permeable Reactive Barriers*, Journal of Hazardous Materials, Vol. 160, PP. 428–434.

El-Sayed, G. O., Dessouki, H. A., and Ibrahim, S. S., 2010, *Bio-sorption of Ni(II) and Cd(II) Ions from Aqueous Solutions onto Rice Straw*, Chemical Science Journal, CSJ-9.

Faisal, A. A., 2006, *Numerical Modeling of Light Non-aqueous Phase Liquid Spill Transport in an Unsaturated-saturated Zone of the Soil*, Ph.D Thesis, Baghdad University, College of Engineering.

Hadjmohammadi, M. R., Salary, M., and Biparva, P., 2011, *Removal of Cr(vi) from Aqueous Solution using Pine Needles Powder as a Bio-sorbent*, Journal of Applied Sciences in Environmental Sanitation, Vol. 6, No. 1, PP. 1-13.

Holzbecher, E., 2007, *Environmental Modeling Using MATLAB*, Springer Berlin Heidelberg New, ISBN: 978-3-540-72936-5.

Plamondon, C. O., Lynch, R., and Al-Tabbaa, A., 2011, *Metal Retention Experiments for the Design of Soil-Mix Technology Permeable Reactive Barriers*, Clean – Soil, Air, Water, Vol. 39, No. 9, PP. 844–852.

Puls, R. W., Powell, R. M., Blowes, D. W., Vogan, J. L., Gillham, R. W., Powell, P.D., Landi, R., Sivavec, T., and Schwltz, D., 1998, *Permeable Reactive Barrier Technologies for Contaminant Remediation*, EPA, 600, (R-98), 125.

Reddi, L. I., and Inyang, H. I., 2000, *Geo-environmental Engineering: Principles and Applications*, Marcel Dekker, Inc, ISBN: 0-8247-0045-7.

Stengele, R. H., and Kohler, S., 2001, *Permeable Reactive Barrier Systems for Groundwater Clean-up*, Geological Survey of Finland, Special paper (32), PP. 175–182.

Ujfaludi, L., 1986, *Longitudinal Dispersion Tests in Non-uniform Porous Media*, Hydrological sciences Journal, Vol. 31, No. 4, PP. 467-474.

Zaiter, M. J., 2006, *Treatment of Low-and Intermediate-Level Radioactive Liquid Waste from Altwath Site using Iraqi Zeolite*, M.Sc. Thesis, Baghdad University.

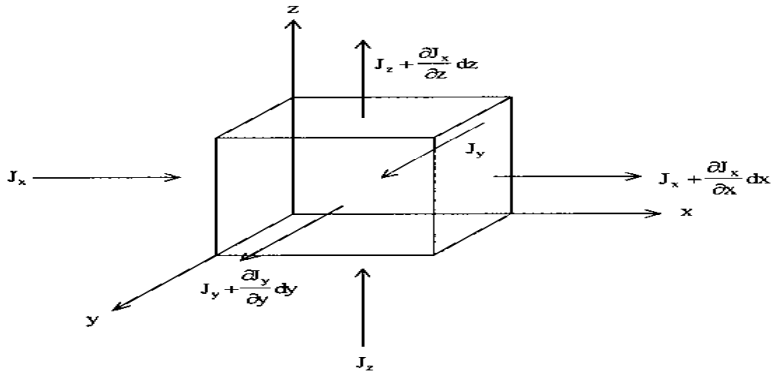

Figure 1. Elemental control volume for mass flux**, Reddi and Inyang, 2000**.

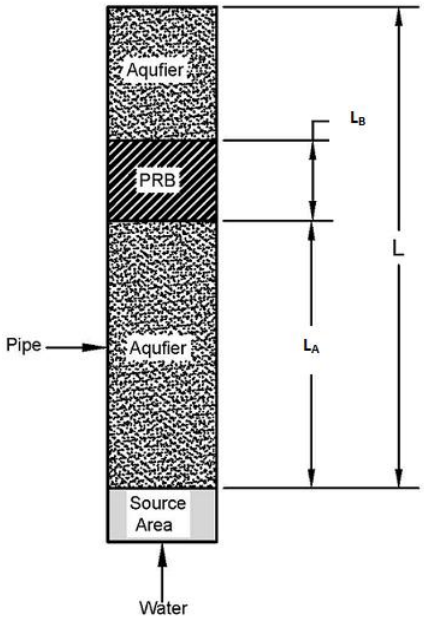

Figure 2. Conceptual model of a contaminant plume passing through a permeable reactive barrier.

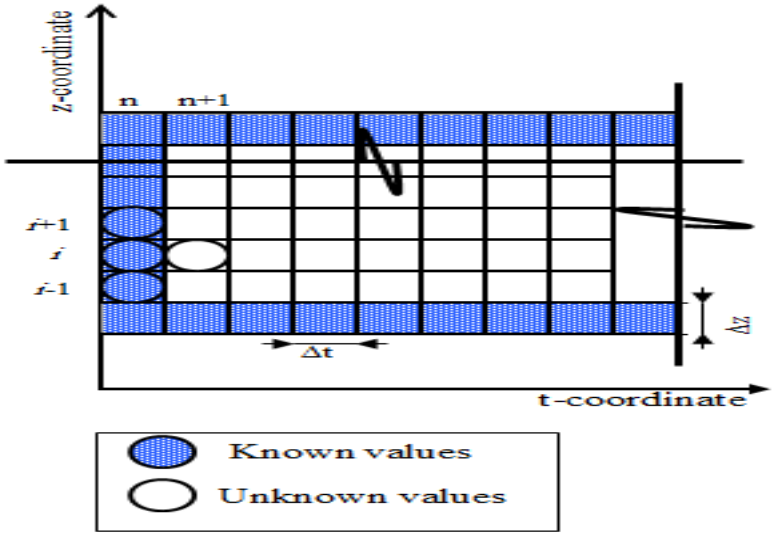

Figure 3. Scheme of spatial and temporal discretization**, Faisal, 2006**.

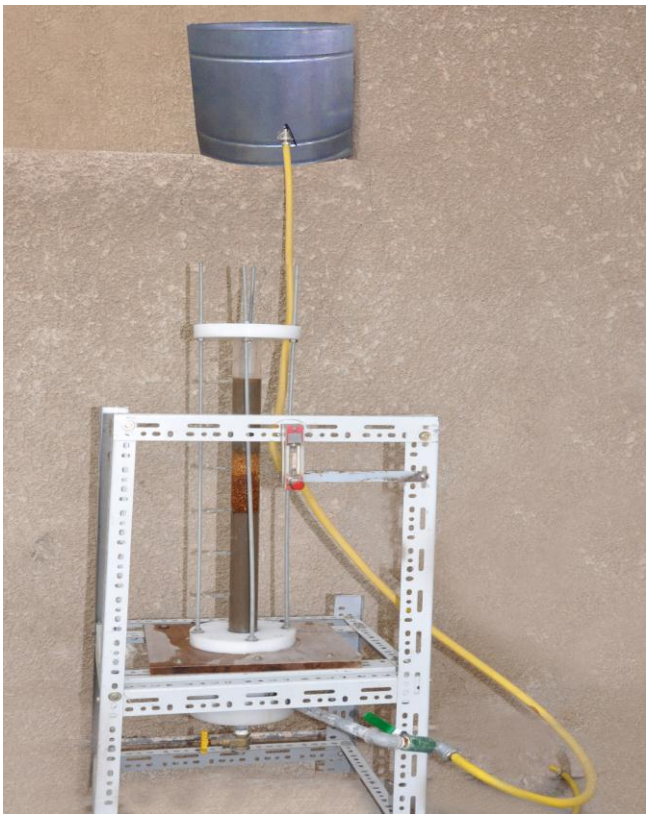

Figure 4. Experimental set-up of column test used in the present study**.**

Table 1. Composition and properties of the soil used in the present study.

Property	Value
Particle size distribution (ASTM D 422) Sand (%) Silt (%) Clay (%)	 90 10 -
Hydraulic conductivity (or coefficient of permeability) (cm s^{-1})	$1.54x10^{-4}$
Cation exchange capacity (meq/100 g)	1.56
pH	7.5
Organic content (ASTM D 2974) (%)	0.26
Bulk density (g/cm^3)	1.29
Porosity (n_A)	0.51
Soil classification	Sand

Table 2. Composition and physico-chemical properties of zeolite.

Property	Percentage (%)
SiO_2	34.48
Al_2O_3	29.94
L.O.I	15.05
Na_2O	13.40
CaO	2.52
TiO_2	1.70
Bulk density (g/cm^3)	0.58
Particle density (g/cm^3)	1.2
Porosity (n_B)	0.34
Surface area (m^2/g)	1000
Cation exchange capacity (meq/100 g)	1.8

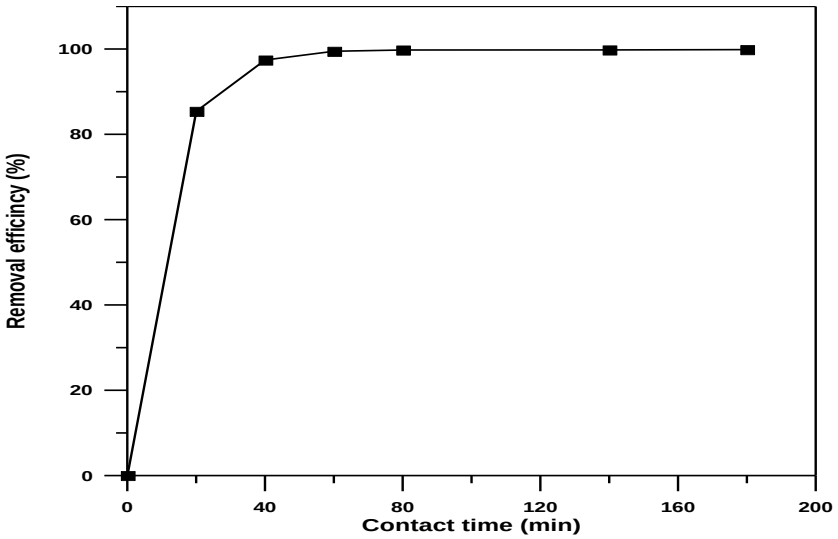

Figure 5. Removal efficiency of cadmium on zeolite as a function of contact time (pH= 6.5; c_o= 50 mg/l; dose=0.25 g; speed= 270 rpm; T= 25±1^{o}C).

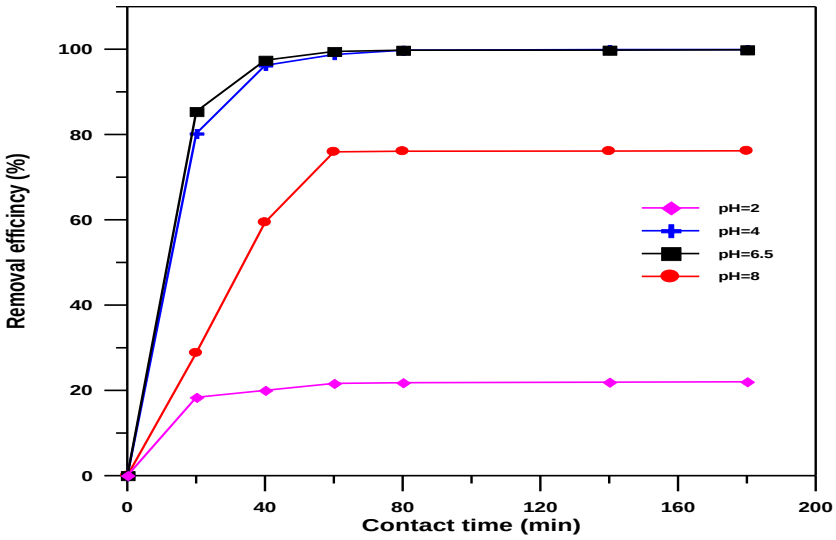

Figure 6. Effect of initial pH on removal efficiency of cadmium on zeolite as a function of contact time (c_o= 50 mg/l; dose=0.25 g; speed= 270 rpm; T= 25±1^{o}C).

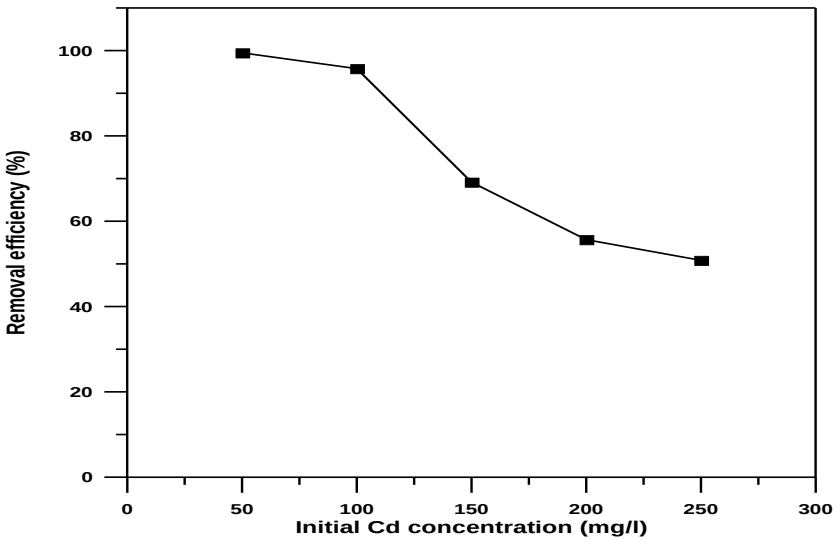

Figure 7. Effect of initial concentration on removal efficiency of cadmium on zeolite (pH=6.5; dose=0.25 g; speed= 270 rpm; contact time=1 h; T= 25±1^{o}C).

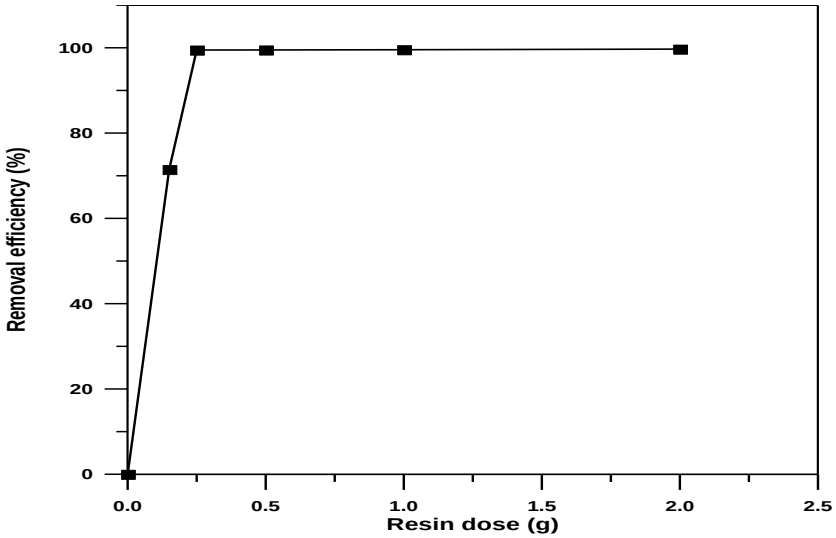

Figure 8. Effect of resin dosage on removal efficiency of cadmium (c_o=50 mg/l; pH=6.5; speed= 270 rpm; contact time=1 h; T= 25±1^{o}C)

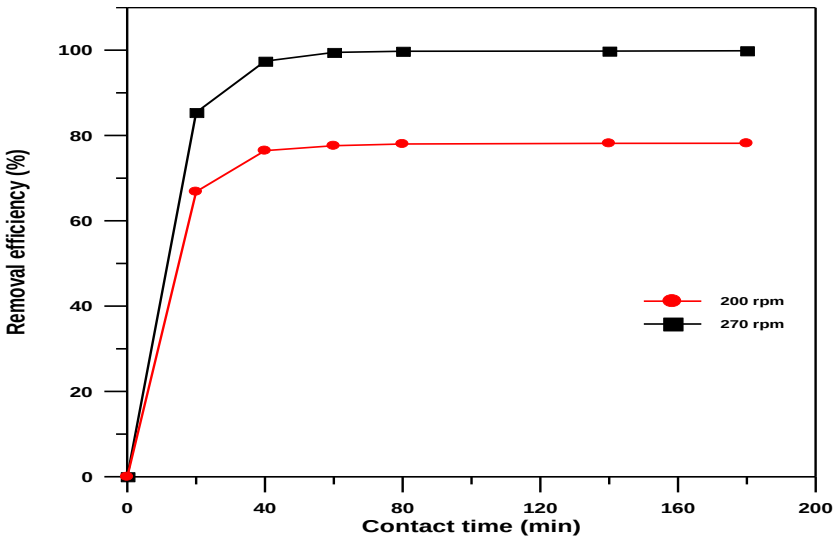

Figure 9. Effect of agitation speed on removal efficiency of cadmium as a function of contact time (c_o=50 mg/l; pH=6.5; resin dose= 0.25 g/100 ml; T= 25±1^{o}C)

Table 3. Experimental equilibrium data of cadmium on zeolite resin (pH=6.5; resin dose= 0.25 g/100 ml; agitation speed= 270 rpm; contact time=1 h; T= 25±1^{o}C).

Initial Con. (c_o) (mg/l)	**Equilibrium Con. (c_e) (mg/l)**	**Sorbed Con. (q_e) (mg/g)**
50	0.255	19.9
100	4.22	38.3
150	46.26	41.5
200	88.66	44.5
250	122.93	50.8

Table 4. Measured values of the longitudinal dispersion coefficient for used mediums as a function of mean pore velocity.

Sand Soil	V (cm/s)	0.00903	0.01806	0.02709
	D_L (cm^2/s)	0.490	0.567	0.670
Zeolite	V (cm/s)	0.0135	0.0270	0.0406
	D_L (cm^2/s)	0.199	0.53	0.66

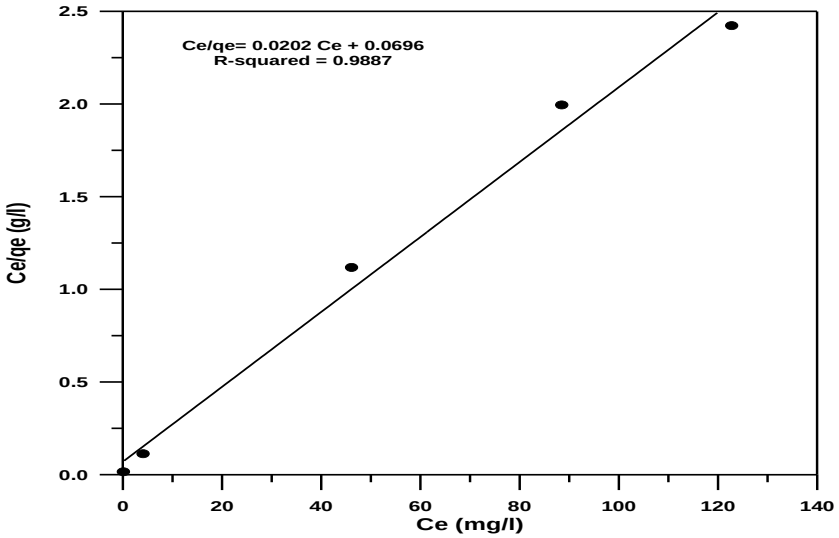

Figure 10. Langmuir isotherm for ion exchange of cadmium on zeolite (pH=6.5; resin dose= 0.25 g/100 ml; agitation speed= 270 rpm; contact time=1 h; T= 25±1^{o}C).

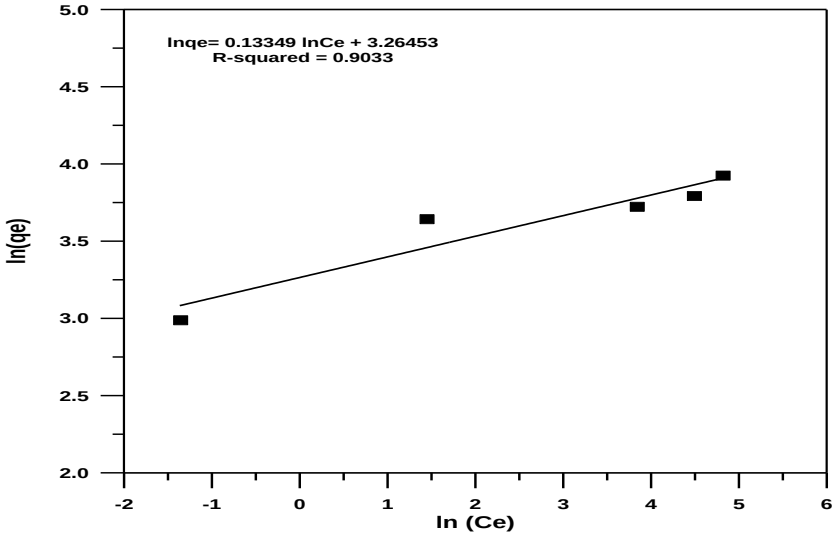

Figure 11. Freundlich isotherm for ion exchange of cadmium on zeolite (pH=6.5; resin dose= 0.25 g/100 ml; agitation speed= 270 rpm; contact time=1 h; T= 25±1^{o}C).

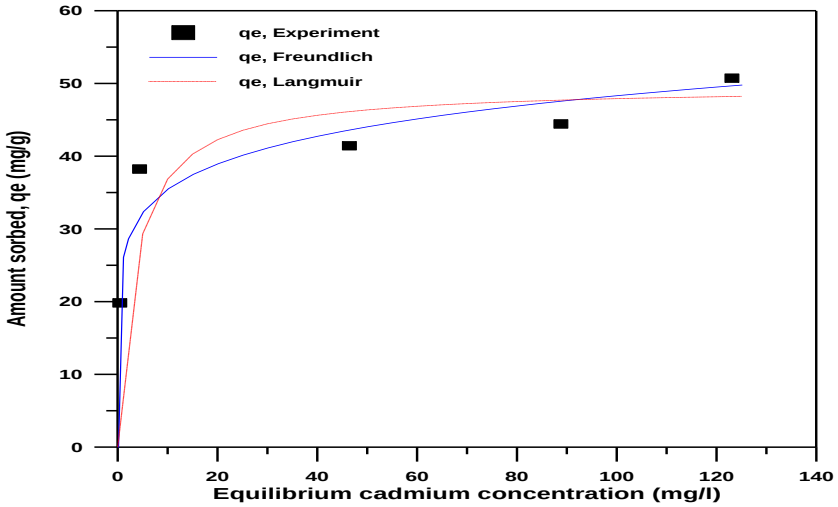

Figure 12. Comparison of the experimental results with the q_e values obtained by two isotherm models for Cd^{2+} removal by zeolite.

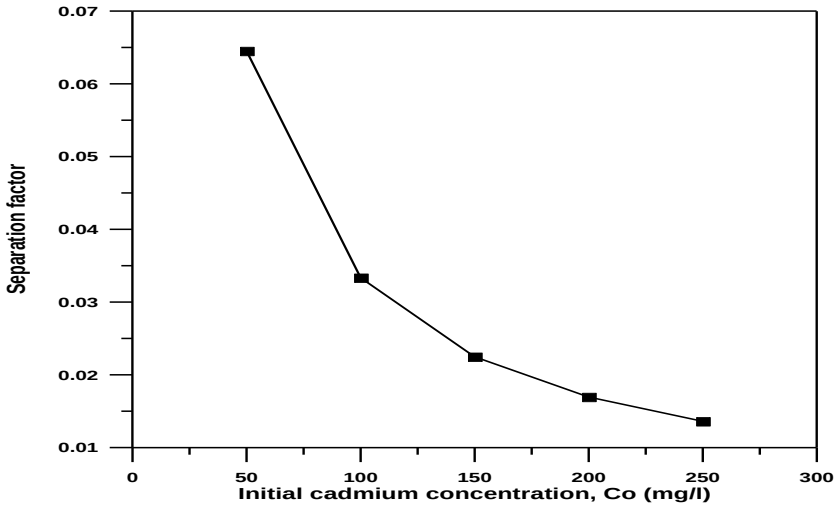

Figure 13. Variation of adsorption intensity with initial cadmium concentration on zeolite resin**.**

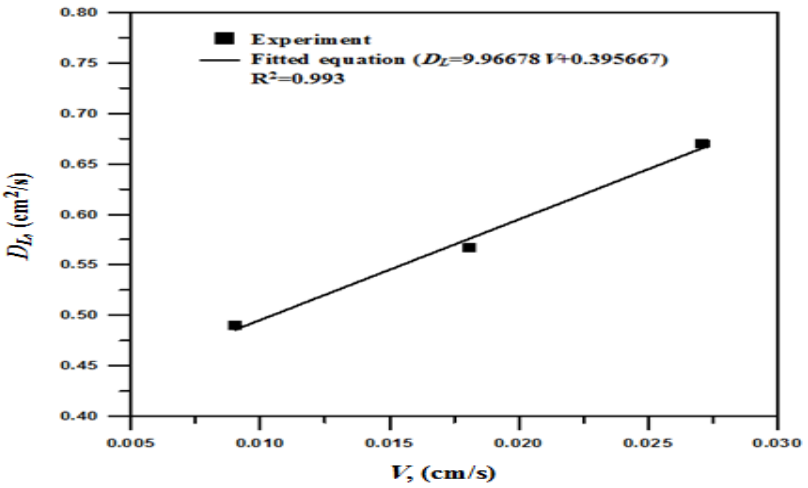

Figure 14. Longitudinal dispersion coefficient versus mean pore velocity relation for sand soil.

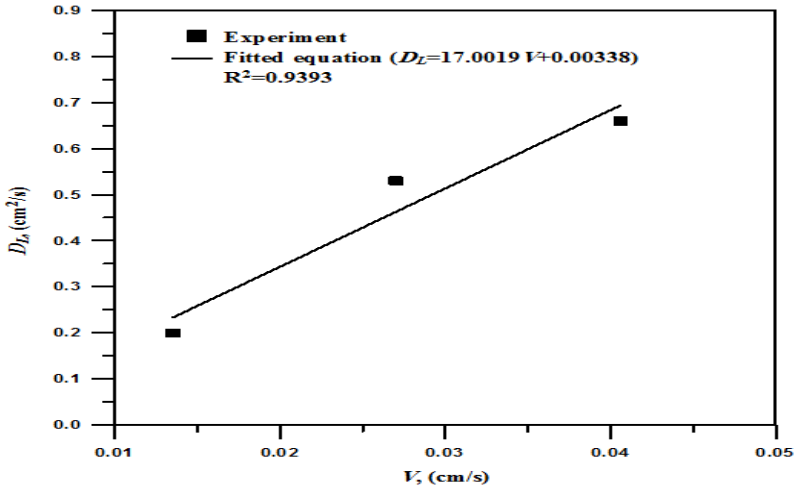

Figure 15. Longitudinal dispersion coefficient versus mean pore velocity relation for zeolite resin.

Table 5. Calculated values of the longitudinal dispersivity and molecular diffusion coefficient for used mediums as a function of mean pore velocity.

Sand Soil	V (cm/s)	0.00903	0.01806	0.02709
	α_L (cm)	9.96678	9.96678	9.96678
Zeolite	V (cm/s)	0.0135	0.0270	0.0406
	α_L (cm)	17.0019	17.0019	17.0019

Table 6. Calculated values of retardation factor dependent on Langmuir sorption isotherm.

Initial Con. (c_o) (mg/l)	**Equilibrium Con. (c_e=c_{cdB}) (mg/l)**	R_L
50	0.255	13883
100	4.22	3238
150	46.26	78
200	88.66	23
250	122.93	13

Table 7. Summary of PRB application example parameters.

Item	Parameter	Value or description
Aquifer characteristics	Aquifer bed depth before barrier (cm)	45
	Aquifer bed depth after barrier (cm)	15
	Porosity of aquifer (n_A)	0.51
	Longitudinal dispersivity (α_L, cm)	9.96678
	Bulk density (g/cm^3)	1.29
	Particle density (g/cm^3)	2.65
PRB characteristics	Adsorbing medium	zeolite
	Barrier bed depth (cm)	5
	Porosity of barrier (n_B)	0.34
	Longitudinal dispersivity (α_L, cm)	17.0019
	Bulk density (g/cm^3)	0.58
	Particle density (g/cm^3)	1.2
Numerical model parameters	Number of nodes	65
	Time step size (min)	0.001
	Initial concentration of Cd^{+2} (mg/l)	zero
Boundary conditions	Concentration of Cd^{+2} @ z=0 (mg/l)	50
	$\frac{\partial c_{cd}}{\partial z}$ at $z_{0=65\ cm}$	zero

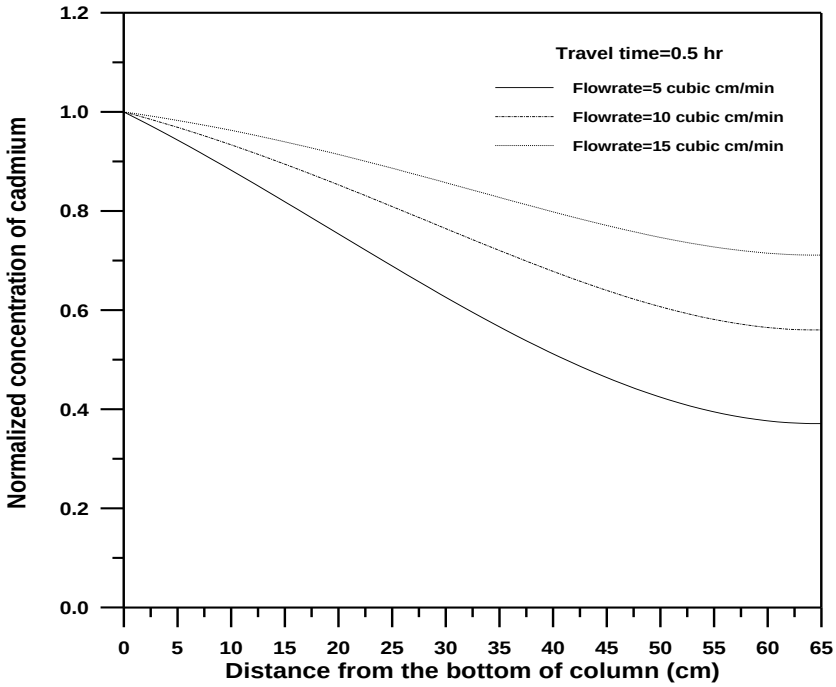

Figure 16. Cadmium concentration distribution in the groundwater along the length of the soil column without using PRB after 0.5 hr.

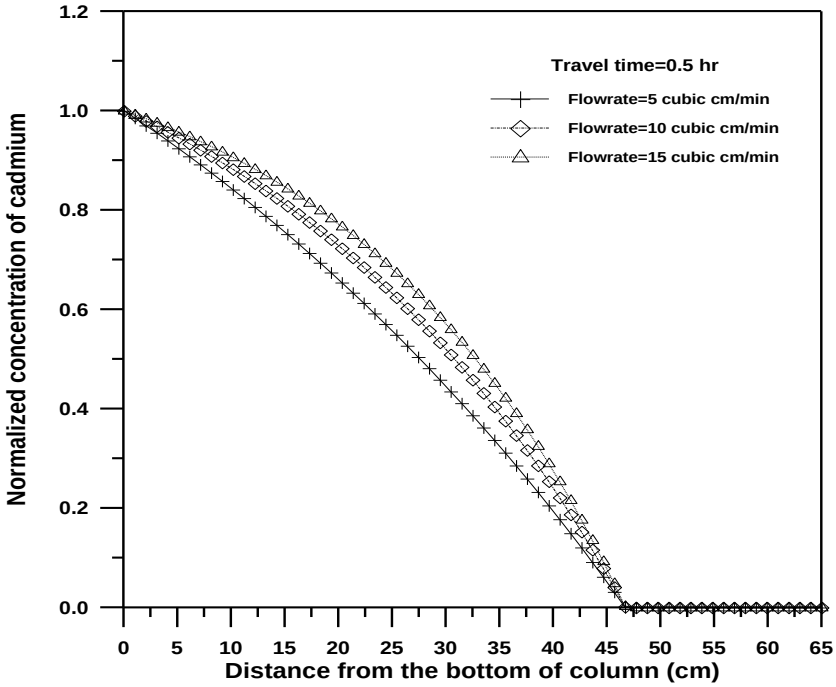

Figure 17. Cadmium concentration distribution in the groundwater along the length of the soil column with using PRB after 0.5 hr.

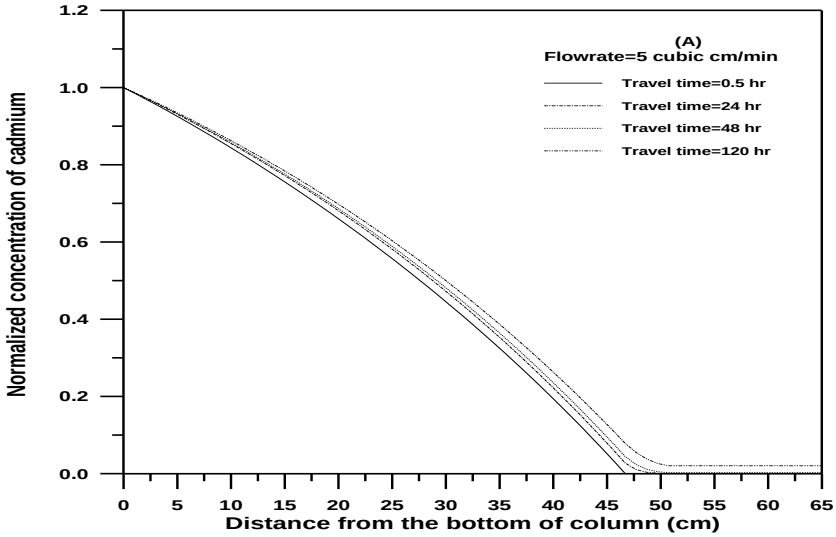

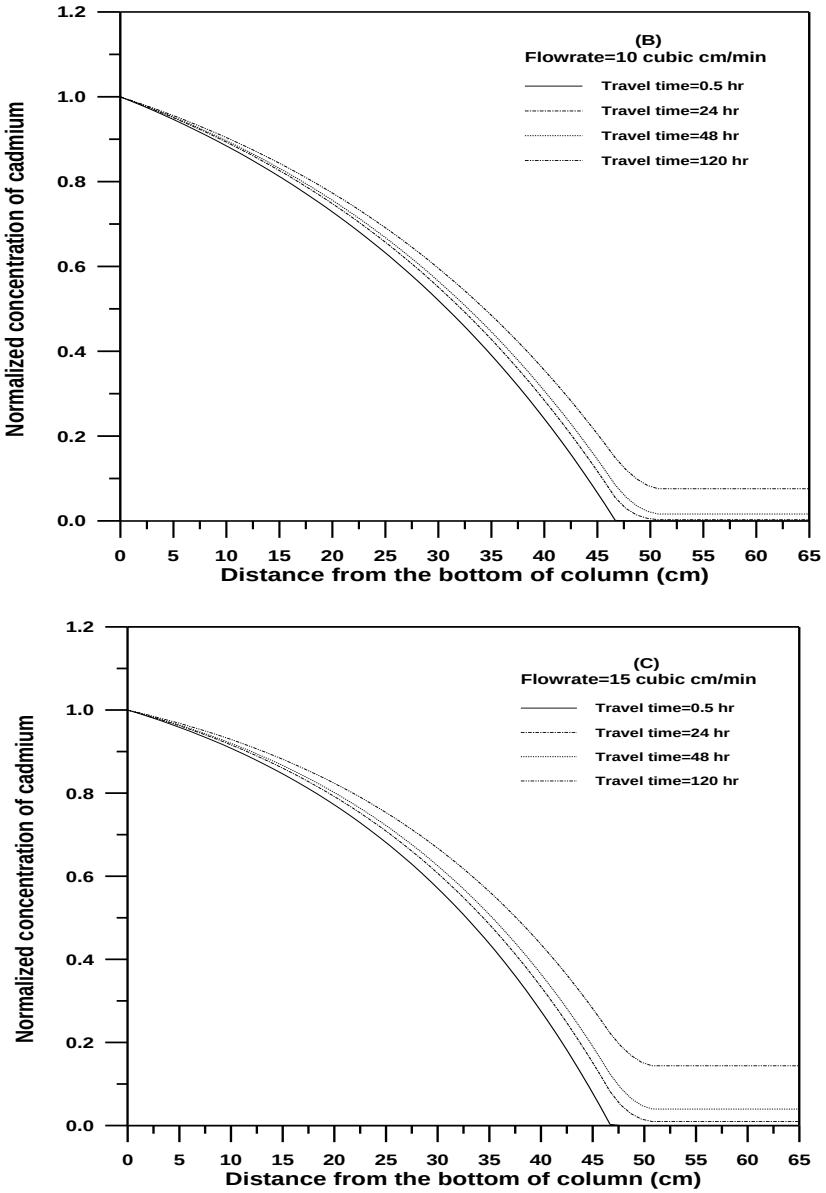

Figure 18. Cadmium concentration distribution in the groundwater along the length of the soil column with using PRB at different time intervals for flow rate equal to (A) 5, (B) 10, (C) 15

cm^3/min.

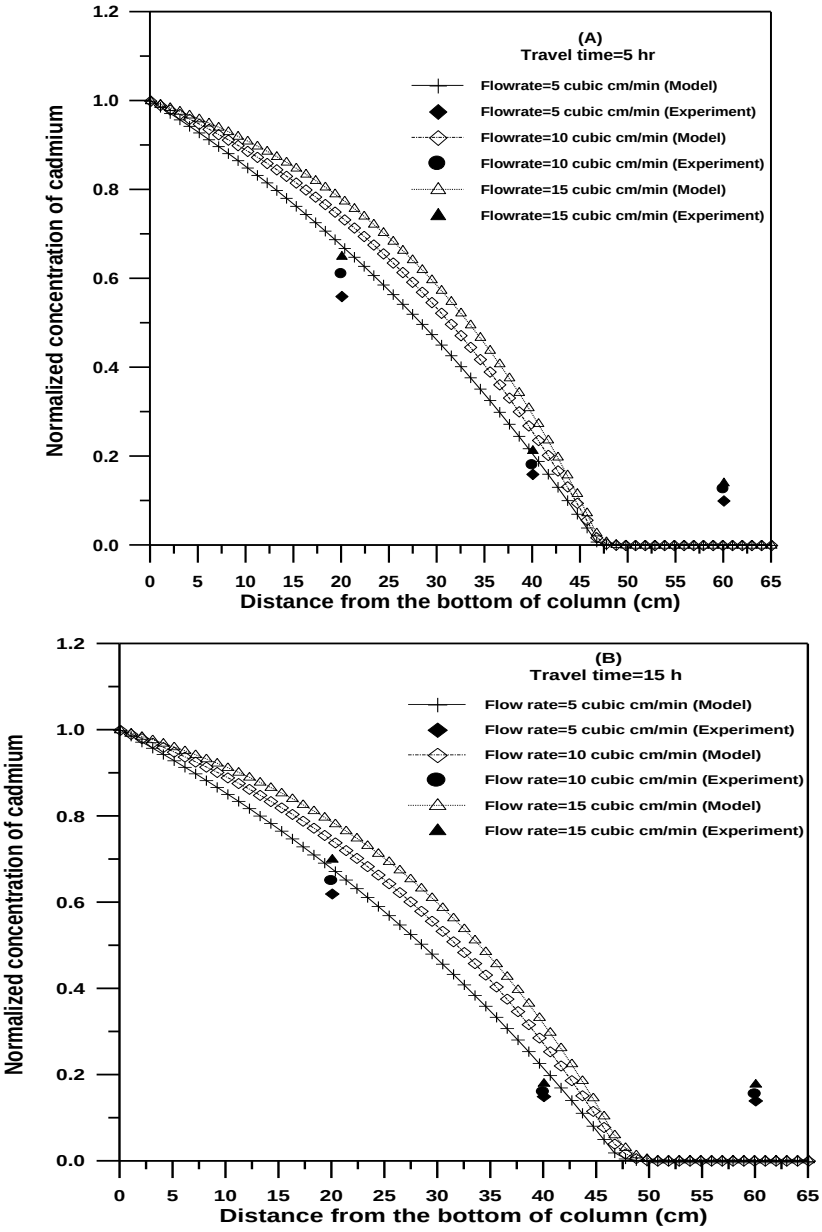

Figure 19. Comparison between model predictions and experimental results for Cd^{+2} concentrations in groundwater for travel time equal to (A) 5 hr and (B) 15 hr.